Inorg. Chem. **2008**, *47*, 11305−11313

Synthesis of N-Confused Tetraphenylporphyrin Rhodium Complexes Having Versatile Metal Oxidation States

Alagar Srinivasan,[†] Motoki Toganoh,[†] Teppei Niino,[†] Atsuhiro Osuka,[‡] and Hiroyuki Furuta*[,†,§]

Department of Chemistry and Biochemistry, Graduate School of Engineering, Kyushu University, 744 Motooka, Nishi-ku, Fukuoka 819-0395, Japan, Department of Chemistry, Graduate School of Science, Kyoto University, Kyoto 606-8502, Japan, and PRESTO, Japan Science and Technology Agency, 4-1-8 Honcho, Kawaguchi 332-0012, Japan

Received June 17, 2006

A variety of N-confused tetraphenylporphyrin rhodium complexes were synthesized, and their structures and physical properties were investigated. Depending on the reaction conditions, the rhodium(I), -(III), and -(IV) complexes were produced, which exemplified the versatile coordination mode of N-confused porphyrin ligands.

Introduction

Porphyrin metal complexes continue to play important roles in the field of bioorganic chemistry, materials science, and catalyst.[1] An endless number of porphyrin metal complexes have been synthesized, and almost all metals in a periodic table are used in this area. Despite such a spread, structural diversity is extremely poor. Because all of the nitrogen atoms point inside the macrocyclic ring, almost all of the complexes have the type A structure (Scheme 1). While some peripherally coordinated organometallic complexes (type B) were prepared in the past decade,[2] such examples were very limited.

Confusion of one pyrrole ring in a porphyrin core dramatically changes the situation.[3] In N-confused porphyrin (denoted as NCP),[4] one nitrogen atom points outside the macrocyclic ring and has an "opened" structure in contrast to a "closed" normal porphyrin. Now we can easily imagine a variety of metal complexes bearing an NCP ligand like types I−IV as shown in Scheme 1. Furthermore, synergy of outer and inner coordination could afford supramolecular complexes like types V and

Scheme 1. Structural Diversity of Porphyrin and N-Confused Porphyrin Metal Complexes

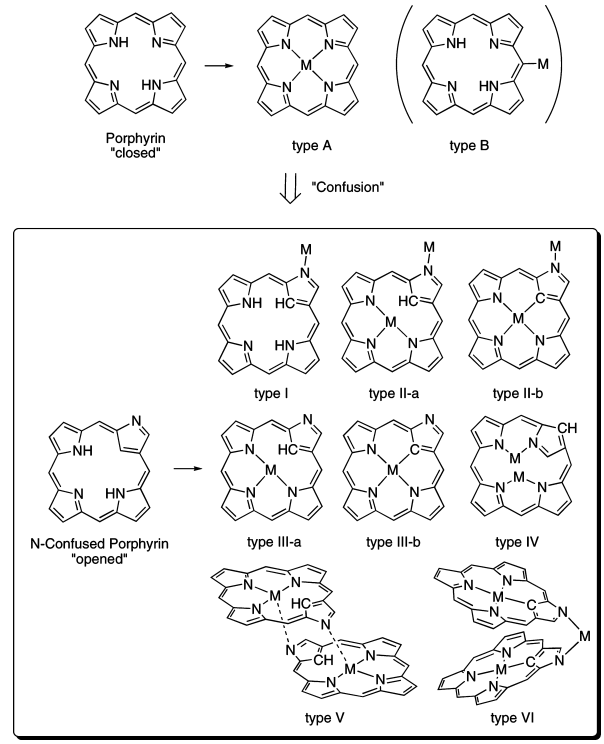

* To whom correspondence should be addressed. E-mail: hfuruta@cstf.kyushu-u.ac.jp.
† Kyushu University.
‡ Kyoto University.
§ PRESTO, Japan Science and Technology Agency.

(1) (a) Smith, K. M. *Porphyrins and Metalloporphyrins*; Elsevier: Amsterdam, The Netherlands, 1975. (b) Kadish, K. M.; Smith, K. M.; Guilard, R. *The Porphyrin Handbook*; Academic Press: San Diego, 2000.
(2) (a) Arnold, D. P.; Sakata, Y.; Sugiura, K.-i.; Worthington, E. I. *Chem. Commun.* **1998**, 2331. (b) Arnold, D. P.; Healy, P. C.; Hodgson, M. J.; Williams, M. L. *J. Organomet. Chem.* **2000**, *607*, 41. (c) Hartnell, R. D.; Arnold, D. P. *Eur. J. Inorg. Chem.* **2004**, 1262.
(3) (a) Lash, T. D. *Synlett* **1999**, 279. (b) Furuta, H.; Maeda, H.; Osuka, A. *Chem. Commun.* **2002**, 1795. (c) Harvey, J. D.; Ziegler, C. J. *Coord. Chem. Rev.* **2003**, *247*, 1. (d) Sessler, J. L.; Seidel, D. *Angew. Chem., Int. Ed.* **2003**, *42*, 5134. (e) Chandrashekar, T. K.; Venkatraman, S. *Acc. Chem. Res.* **2003**, *36*, 676. (f) Ghosh, A. *Angew. Chem., Int. Ed.* **2004**, *43*, 1918. (g) Stępień, M.; Latos-Grażyński, L. *Acc. Chem. Res.* **2005**, *38*, 88. (h) Chmielewski, P. J.; Latos-Grażyński, L. *Coord. Chem. Rev.* **2005**, *249*, 2510. (i) Srinivasan, A.; Furuta, H. *Acc. Chem. Res.* **2005**, *38*, 10. (j) Harvey, J. D.; Ziegler, C. J. *J. Inorg. Biochem.* **2006**, *100*, 869.

10.1021/ic061093+ CCC: $40.75
Published on Web 10/28/2008

VI. Such versatility of the NCP ligand has already been demonstrated in manganese,[5] iron,[6] cobalt,[7] nickel,[4b,8] copper,[9] zinc,[10] molybdenum,[11] palladium,[12] silver,[9,13] cadmium,[10b] antimony,[14] rhenium,[15] iridium,[16] platinum,[17] mercury,[10b] erbium,[18] and ytterbium[18] complexes. Previously, we have shown the formation of a bisrhodium(I) complex of type II.[19] Here, rhodium chemistry of N-confused tetraphenylporphyrin (NCTPP) was extensively investigated, and we succeeded to prepare metal complexes of types I−III (Scheme 2). Treatment of NCTPP with 0.5 equiv of $[RhCl(CO)_2]_2$ gave a rhodium(I) complex **1** (type I). When 1.0 equiv of $[RhCl(CO)_2]_2$ was used in the presence of a base, bisrhodium(I) complex **2** (type II) was obtained. The reaction of **2** with pyridine or I_2 afforded a rhodium(III) complex **3** or a rhodium(IV) complex **4**, respectively (type III). Further treatment of **3** with 0.5 equiv of $[RhCl(CO)_2]_2$ gave mixed-valence binuclear complex **5** (type II). The properties of NCTPP rhodium complexes were studied, and a comparison with those of tetraphenylporphyrin (TPP) complexes was discussed.

Results and Discussion

Type I complex bearing an NCTPP ligand was readily available essentially in a quantitative yield by the treatment of NCTPP with a dimeric rhodium(I) compound (Scheme 3). Upon treatment of NCTPP with 0.5 equiv of $[RhCl(CO)_2]_2$in CH_2Cl_2 at ambient temperature, coordination of NCTPP to the rhodium metal occurred immediately (within 10 min). The ^1H NMR analysis on the crude product indicated that only the single product was obtained under these conditions. After recrystallization from CH_2Cl_2/hexane, the rhodium(I) complex **1** was isolated in 93% yield as a greenish-brown solid. The rhodium complex **1** was rather stable and did not decompose on exposure to air and sunlight in a $CDCl_3$ solution for 2 weeks. The structure of **1** was determined by spectroscopic methods. The high-resolution mass analysis (ESI^+) gave acceptable results ($[MH]^+$: found, 809.1227; calcd, 809.1191). Strong absorptions

Scheme 2. Formation of NCTPP Rhodium Complexes

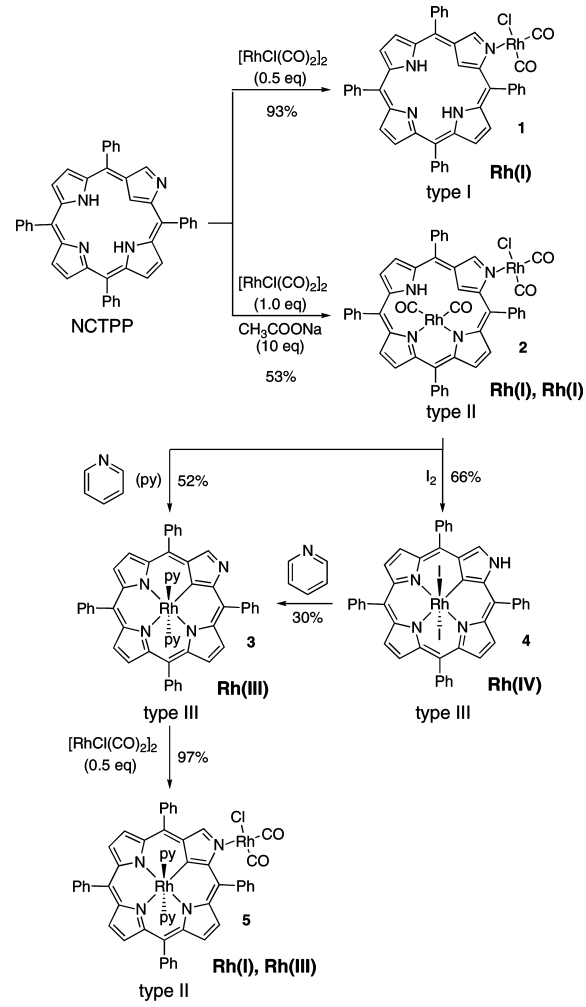

Scheme 3. Preparation of **1**

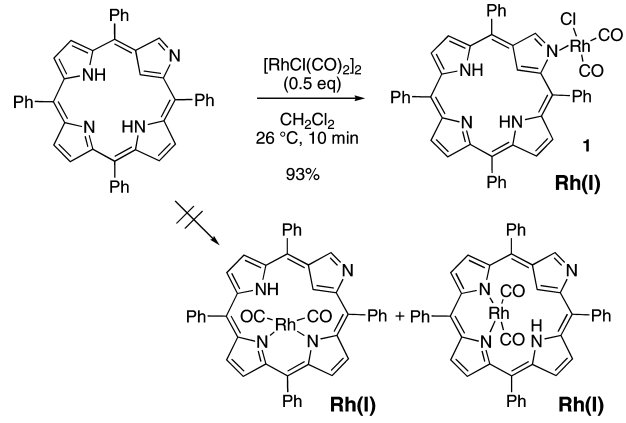

(4) (a) Furuta, H.; Asano, T.; Ogawa, T. *J. Am. Chem. Soc.* **1994**, *116*, 767. (b) Chmielewski, P. J.; Latos-Grażyński, L.; Rachlewicz, K.; Głowiak, T. *Angew. Chem., Int. Ed. Engl.* **1994**, *33*, 779.

(5) (a) Bohle, D. S.; Chen, W.-C.; Hung, C.-H. *Inorg. Chem.* **2002**, *41*, 3334. (b) Harvey, J. D.; Ziegler, C. J. *Chem. Commun.* **2002**, 1942. (c) Harvey, J. D.; Ziegler, C. J. *Chem. Commun.* **2003**, 2890.

(6) (a) Chen, W.-C.; Hung, C.-H. *Inorg. Chem.* **2001**, *40*, 5070. (b) Hung, C.-H.; Chen, W.-C.; Lee, G.-H.; Peng, S.-M. *Chem. Commun.* **2002**, 1516. (c) Hung, C.-H.; Chang, C.-H.; Ching, W.-M.; Chuang, C.-H. *Chem. Commun.* **2006**, 1866.

(7) Harvey, J. D.; Ziegler, C. J. *Chem. Commun.* **2004**, 1666.

(8) Chmielewski, P. J.; Schmidt, I. *Inorg. Chem.* **2004**, *43*, 1885.

(9) (a) Chmielewski, P. J.; Latos-Grażyński, L.; Schmidt, I. *Inorg. Chem.* **2000**, *39*, 5475. (b) Maeda, H.; Osuka, A.; Ishikawa, Y.; Aritome, I.; Hisaeda, Y.; Furuta, H. *Org. Lett.* **2003**, *5*, 1293.

(10) (a) Furuta, H.; Ishizuka, T.; Osuka, A. *J. Am. Chem. Soc.* **2002**, *124*, 5622. (b) Furuta, H.; Morimoto, T.; Osuka, A. *Inorg. Chem.* **2004**, *43*, 1618. (c) Morimoto, T.; Uno, H.; Furuta, H. *Angew. Chem., Int. Ed.* **2007**, *46*, 3672. (d) Toganoh, M.; Harada, N.; Morimoto, T.; Furuta, H. *Chem.—Eur. J.* **2007**, *13*, 2257.

(11) Harvey, J. D.; Shaw, J. L.; Herrick, R. S.; Ziegler, C. J. *Chem. Commun.* **2005**, 4663.

(12) Furuta, H.; Kubo, N.; Maeda, H.; Ishizuka, T.; Osuka, A.; Nanami, H.; Ogawa, T. *Inorg. Chem.* **2000**, *39*, 5424.

(13) (a) Furuta, H.; Ogawa, T.; Uwatoko, Y.; Araki, K. *Inorg. Chem.* **1999**, *38*, 2676. (b) Chmielewski, P. J. *Angew. Chem., Int. Ed.* **2005**, *44*, 6417.

(14) (a) Ogawa, T.; Furuta, H.; Takahashi, M.; Morino, A.; Uno, H. *J. Organomet. Chem.* **2000**, *61*, 551. (b) Liu, J.-C.; Ishizuka, T.; Osuka, A.; Furuta, H. *Chem. Commun.* **2003**, 1908.

(15) (a) Toganoh, M.; Ishizuka, T.; Furuta, H. *Chem. Commun.* **2004**, 2464. (b) Toganoh, M.; Furuta, H. *Chem. Lett.* **2005**, 1034. (c) Toganoh, M.; Ikeda, S.; Furuta, H. *Chem. Commun.* **2005**, 4589. (d) Toganoh, M.; Ikeda, S.; Furuta, H. *Inorg. Chem.* **2007**, *46*, 10003.

(16) Toganoh, M.; Konagawa, J.; Furuta, H. *Inorg. Chem.* **2006**, *45*, 3852.

(17) (a) Furuta, H.; Youfu, K.; Maeda, H.; Osuka, A. *Angew. Chem., Int. Ed.* **2003**, *42*, 2186. (b) Chmielewski, P. J.; Schmidt, I. *Inorg. Chem.* **2004**, *43*, 1885.

(18) Zhu, X.; Wong, W.-K.; Lo, W.-K.; Wong, W.-Y. *Chem. Commun.* **2005**, 1022.

(19) (a) Precedent communication: Srinivasan, A.; Furuta, H.; Osuka, A. *Chem. Commun.* **2001**, 1666. (b) Please also see: Toganoh, M.; Niino, T.; Maeda, H.; rioletti, B.; Furuta, H. *Inorg. Chem.* **2006**, *45*, 10428.

Scheme 4. Preparation of **2** and **6**

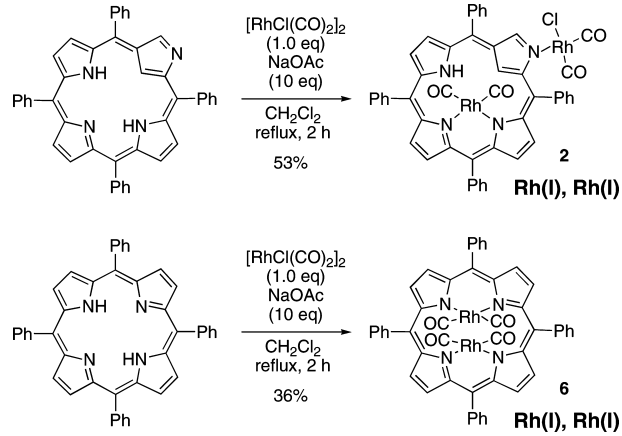

due to carbonyl stretching were observed at 2071 and 1995 cm^{-1} in the IR spectrum. The ^1H NMR spectrum as well as the ^{13}C NMR spectrum was fully consistent with the assigned structure. For example, a sharp singlet signal due to inner CH and a broad signal due to inner NH were observed at δ −4.64 and −1.81 ppm, respectively, in the ^1H NMR spectrum. The $^{103}Rh-^{13}C$ coupling constants between the rhodium center and the carbonyl groups, which were determined by ^{13}C NMR measurement, were typical for rhodium carbonyl complexes ($^1J_{Rh-C}$ = 72.2 Hz at δ 180.52 ppm; $^1J_{Rh-C}$ = 66.6 Hz at δ 183.83 ppm). Furthermore, X-ray photoelectron spectroscopy analysis indicated the presence of rhodium, nitrogen, and chlorine atoms in a 1:4:1 ratio from the integrated area of the corresponding peaks.

At this stage, coordination of a rhodium metal occurred preferentially at the peripheral nitrogen atom.[20] Even when the reaction of NCTPP with 0.5 equiv of $[RhCl(CO)_2]_2$ was achieved under basic conditions, the peripherally coordinated complex **1** was detected as a major product in ^1H NMR analysis.[21] While internally coordinated rhodium carbonyl complexes were often observed in other porphyrinoid systems,[19,22] monorhodium(I) complexes of such types were not isolated yet in the case of NCP.

Type II complex was obtained from the reaction of NCTPP with 1.0 equiv of $[RhCl(CO)_2]_2$ in the presence of 10 equiv of NaOAc (Scheme 4). The reaction proceeded smoothly under reflux conditions in CH_2Cl_2 to give, after silica gel column separation, the bisrhodium(I) complex **2** in 53% yield. A smaller amount of the rhodium reagent caused predominant production of the monorhodium complex **1**, and use of an excess amount of the rhodium reagent gave no significant effect. While the rhodium complex **2** was rather stable in the solid state, it was slowly decomposed in solution at ambient temperature presumably via insertion of the interior rhodium metal to the inner C−H bond. The assigned structure of **2** rested on the mass, ^1H NMR, and IR spectra and was subsequently confirmed by the X-ray crystallographic analysis. In the mass analysis, the reasonable peaks were observed by either electrospray ionization (ESI; $[M - Cl]^+$ = 931) or fast atom bombardment (FAB; $[MH]^+$ = 967) modes. The IR spectrum (2075, 2010, and 1993 cm^{-1}) clearly showed the presence of carbonyl groups. The signals due to the inner hydrogen atoms connected to the carbon atom (δ −3.83 ppm) and the nitrogen atom (δ 0.11 ppm) were observed distinctly in the ^1H NMR spectrum. The reaction of TPP under similar conditions gave the corresponding bisrhodium(I) complex **6** in 36% yield.

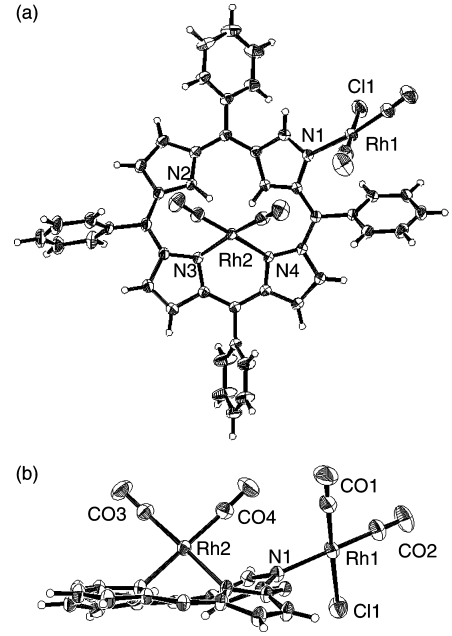

Figure 1. Molecular structures of **2**·0.5CH_2Cl_2·0.5H_2O with 30% probability level ellipsoids: (a) top view; (b) side view. The phenyl groups in the side view and solvent molecules are omitted for clarity (figures are redrawn from the data of ref19).

Table 1. Selected Bond Lengths (Å) and Angles (deg) of the Rhodium Complex **2**

Rh1−N1	2.104(3)	N1−Rh1−Cl1	87.58(9)
Rh1−Cl1	2.349(1)	Cl1−Rh1−CO2	86.8(2)
Rh1−CO1	1.839(5)	CO2−Rh1−CO1	91.0(2)
Rh1−CO2	1.843(5)	CO1−Rh1−N1	94.5(2)
Rh2−N3	2.098(3)	N3−Rh2−N4	85.6(2)
Rh2−N4	2.076(3)	N4−Rh2−CO4	91.7(2)
Rh2−CO3	1.858(4)	CO4−Rh2−CO3	89.6(2)
Rh2−CO4	1.860(4)	CO3−Rh2−N3	93.0(2)

Explicit structural details were derived from the X-ray crystallographic analysis. The ORTEP diagram of **2** is shown in Figure 1, and the bond lengths and angles around the metal centers are summarized in Table 1. Evidently, two rhodium metals are attached to one NCTPP skeleton; one rhodium metal (Rh1) is attached to the peripheral nitrogen atom (N1), and the other rhodium metal (Rh2) is attached to two of the three inner nitrogen atoms (N3 and N4). The Rh1 ion has the chloride ligand and the two carbonyl ligands in addition to the imino nitrogen atom of the NCTPP core, suggesting that the formal charge on the Rh1 ion is 1+. The Rh2 ion has the two carbonyl ligands in addition to the imino and amino nitrogen atoms of the NCTPP core. The structure

(20) This type of coordination was also suggested in core-modified rubyrin systems: Narayanan, S. J.; Sridevi, B.; Chandrashekar, T. K.; Englich, U.; Ruhlandt-Senge, K. *Inorg. Chem.* **2001**, *40*, 1637.

(21) Because the rhodium complex **1** was decomposed during silica gel column separation, it was difficult to determine the precise yield. The estimated yield from ^1H NMR analysis was ∼80%.

(22) (a) Setsune, J.; Yamauchi, T.; Tanikawa, S. *Chem. Lett.* **2002**, 188. (b) Simkhovich, L.; Rosenberg, S.; Gross, Z. *Tetrahedron Lett.* **2001**, *42*, 4929. (c) Sridevi, B.; Narayanan, S. J.; Rao, R.; Chandrashekar, T. K.; Englich, U.; Ruhlandt-Senge, K. *Inorg. Chem.* **2000**, *39*, 3669. (d) Sessler, J. L.; Gebauer, A.; Guba, A.; Scherer, M.; Lynch, V. *Inorg. Chem.* **1998**, *37*, 2073. (e) Burrell, A. K.; Sessler, J. L.; Cyr, M. J.; McGhee, E.; Ibers, J. A. *Angew. Chem., Int. Ed. Engl.* **1991**, *30*, 91.

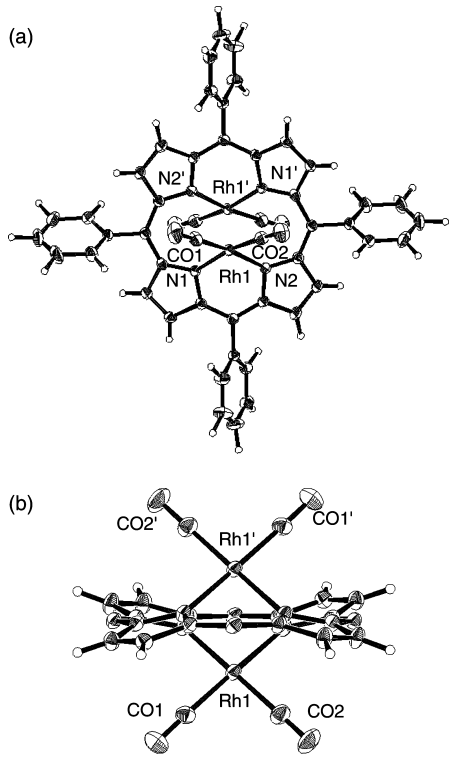

Figure 2. Molecular structures of **6**·CH_2Cl_2 with 30% probability level ellipsoids: (a) top view; (b) side view. The phenyl groups in the side view and solvent molecules are omitted for clarity (figures are redrawn from the data of ref 19).

Table 2. Selected Bond Lengths (Å) and Angles (deg) of the Rhodium Complex **6**

Rh1−N1	2.075(3)	N1−Rh1−N2	84.8(2)
Rh1−N2	2.069(3)	N2−Rh1−CO2	92.5(2)
Rh1−CO1	1.851(5)	CO2−Rh1−CO1	89.9(2)
Rh1−CO2	1.849(4)	CO1−Rh1−N1	92.0(2)

around the Rh2 ion was quite similar to that of the TPP bisrhodium(I) complex (**6**; Figure 2 and Table 2), and the formal charge on the Rh2 ion is 1+.[23] The geometries around the two metal centers are close to square planar (sum of the angles around Rh1 and Rh2 is 359.9° in both cases). While the two rhodium metals are placed on the same side of the porphyrin plane, the distance between the Rh1 ion and the Rh2 ion is quite long (6.286 Å), and hence no significant interaction is expected.

Although two possible isomers would exist as bisrhodium(I) complexes (Figure 3), only isomer A (**2**) was exclusively isolated. Judging from ^{1}H NMR analysis on the crude product before silica gel column chromatography, it mainly contained two compounds in a ratio of ~55:45.[24] Undoubtedly, the major product was isomer A (**2**), and then the minor product was considered to be isomer B because the two compounds show similar signal patterns in the ^{1}H NMR spectrum as well as the absorption spectrum. In density functional theory calculation

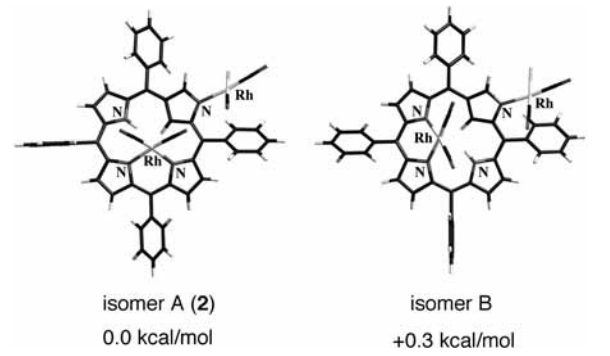

Figure 3. Structures of NCTPP bis-Rh(I) complexes optimized at the B3LYP/631LAN level.

Scheme 5. Possible Mechanism for Isomerization of the NCTPP Bis-Rh(I) Complexes

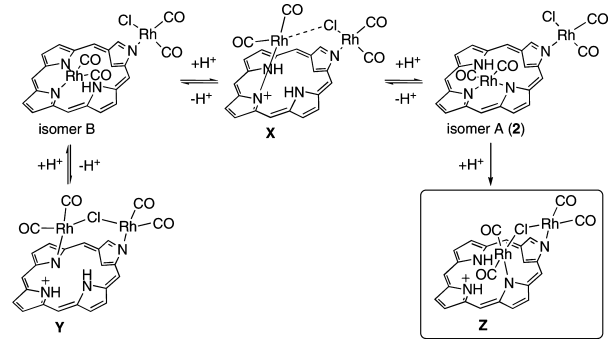

at the B3LYP/631LAN level,[25] isomer A was slightly more stable than isomer B (energy difference: 0.3 kcal/mol), which was well consistent with the isomeric ratio in the crude product. Accordingly, exclusive production of isomer A (**2**) could not be explained simply by a thermodynamic factor. Surprisingly, after the crude product was passed through a pad of silica gel, the signals due to the minor compound had completely disappeared. The weight of the residue after silica gel treatment was not significantly reduced.[26] Thus, SiO_2 would facilitate isomerization from isomer B to isomer A. While no convincing evidence had been obtained yet, we supposed the mechanism of isomerization as shown in Scheme 5. Under weakly acidic conditions on silica gel, protonation to one of the three inner nitrogen atoms occurred to give chlorine-bridged rhodium(I) complex **X**, **Y**, or **Z**.[27] Among the three species, **Z** would be most stable because of the favorable position of the nitrogen atoms and produce preferentially. As a result, after silica gel column separation, only isomer A (**2**) was exclusively obtained. Reproduction of isomer B could be inhibited kinetically. Even after treatment of the isolated isomer A (**2**) with bases such as NaOAc or KO^{t}Bu at ambient temperature, isomer B was not detected in ^{1}H NMR analysis. A similar migration but different

(23) Takenaka, A.; Sasada, Y.; Omura, T.; Ogoshi, H.; Yoshida, Z. *Chem. Commun.* **1973**, 792.
(24) The signals due to inner β-CH were observed at δ −3.82 ppm (minor) and −3.83 ppm (major), respectively. Because all signals were significantly overlapped, it was difficult to determine the product ratio accurately.
(25) The LANL2DZ basis set was used for the rhodium atoms and the 6-31G** basis set for the rest.
(26) Starting from 26.3 mg of NCTPP and 22.6 mg of $[RhCl(CO)_2]_2$, 47.1 mg of the residue was obtained.
(27) Yoshida, Z.; Ogoshi, H.; Omura, T.; Watanabe, E.; Kurosaki, T. *Tetrahedron Lett.* **1972**, 1077.
(28) Mori, S.; Shin, J.-Y.; Shimizu, S.; Ishikawa, F.; Furuta, H.; Osuka, A. *Chem.—Eur. J.* **2005**, *11*, 2417.
(29) Furuta, H.; Ishizuka, T.; Osuka, A.; Dejima, A.; Nakagawa, H.; Ishikawa, Y. *J. Am. Chem. Soc.* **2001**, *123*, 6207.
(30) Jameson, G. B.; Collman, J. P.; Boulatov, R. *Acta Crystallogr., Sect. C* **2001**, *C57*, 406.

Scheme 6. Tautomerism and Type III Metal Coordination of NCTPP

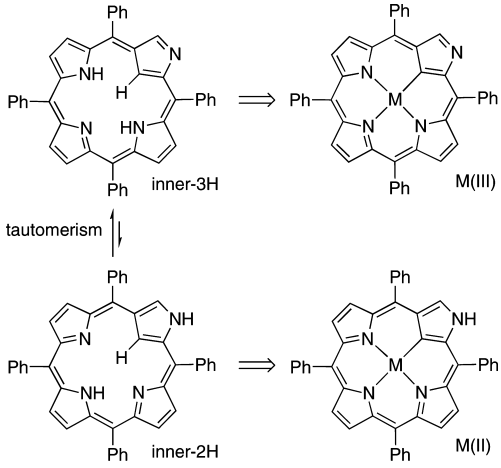

mechanism was reported in the N-fused pentaporphyrin rhodium complexes.[28]

Type III complexes could be prepared by treatment of bisrhodium(I) complex **2** with pyridine or I_2, which showed different reactivities from porphyrin bisrhodium(I) complexes (vide infra). Depending on the axial ligands and tautomeric structure of the NCP ligand (Scheme 6),[29] the rhodium(III) complex **3** and the rhodium(IV) complex **4** were obtained as follows.

When the bisrhodium(I) complex **2** was dissolved in pyridine, a highly polar product was produced immediately, which was confirmed by thin-layer chromatography analysis. After silica gel column purification, the rhodium bispyridine complex **3** was isolated in 52% yield. In the ^{1}H NMR spectrum of **3**, both the sharp singlet signal due to the inner-CH moiety and the broad signal due to the inner-NH moiety of the NCP ligand had disappeared, which indicates that the rhodium atom was wrapped by the porphyrin core. The signals due to the pyridine group appeared at δ 2.36 (ortho), 5.35 (meta), and 6.23 (para) ppm; the ortho protons of the pyridine ligands show a significant upfield shift. This is reasonably explained by the strong shielding effect due to the porphyrin core toward the axial ligands. Furthermore, the broad singlet signal around δ 9.2 ppm, assignable to the outer-NH proton, was not detected, and hence the NCP moiety should have the inner-3H structure, which indicates that the formal charge on the rhodium ion is 3+. This is consistent with the fact that the ^{1}H NMR signals of complex **3** appeared in a normal diamagnetic region. In the ^{13}C NMR spectrum, coupling between the rhodium metal and the inner-carbon atom of the *confused* pyrrole moiety was clearly observed (δ 149.00 ppm, $^1J_{Rh-C} = 26.8$ Hz). Finally, the mass spectrum was consistent with the bispyridine structure (ESI mode $[MH]^+$: found, 873.22295; calcd, 873.22130). It is worth noting that further treatment of **3** with 0.5 equiv of $[RhCl(CO)_2]_2$ afforded the mixed-valence bisrhodium complex **5** in 97% yield in the same manner as the reaction from NCTPP to **1** (Scheme 7). Here, the inner-rhodium atom is trivalent and the outer-rhodium metal is monovalent in the rhodium complex **5**.

To probe the structure of the rhodium complex **3**, an X-ray crystallographic study was conducted on a single crystal grown from CH_2Cl_2/CH_3CN (Figure 4). In the crystal, the rhodium atom is located in the center of the macrocyclic ring and has

Scheme 7. Preparation of **3** and **5**

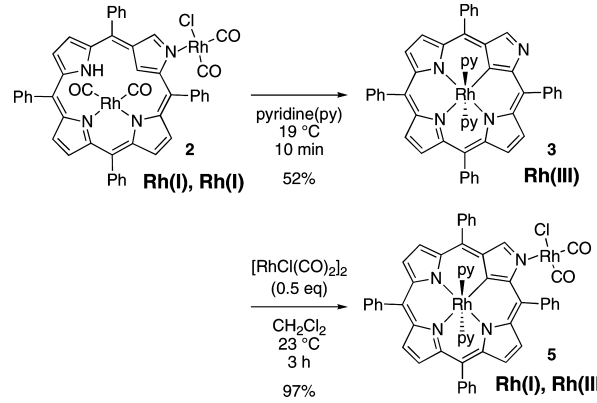

the two axial pyridine ligands; the geometry around the rhodium atom is tetragonal bipyramidal. The distance between the rhodium atom and the axial pyridine ligands is 2.072(3) Å, which is slightly shorter than that of the TPP Rh(III) complex **7** [2.102(7) Å vide infra].[30]

The rhodium(IV) complex **4** was prepared by the reaction of bisrhodium(I) complex **2** with iodine (Scheme 8). The addition of I_2 to **2** caused the production of a less-polar product. After silica gel separation, **4** was obtained in 66% yield. In this reaction, the rhodium(III) complex, which should be a possible intermediate, was not obtained and further oxidation to the rhodium(V) complex was not observed. Because no ^{1}H NMR signals were detected in the regular diamagnetic region (vide infra) and only the fragment peaks were detected in ESI and

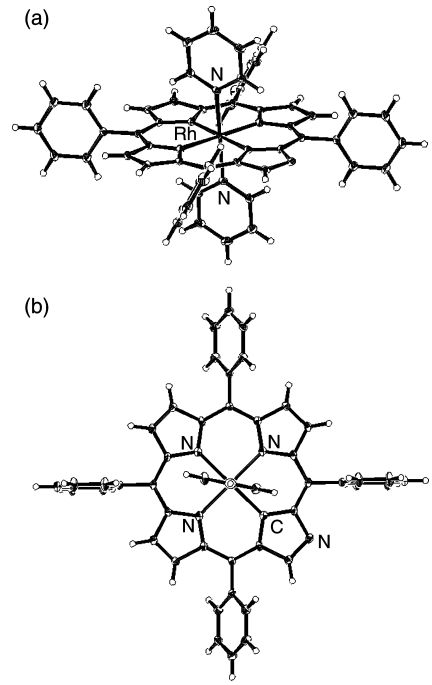

Figure 4. Molecular structures of **3**·2CH_3CN with 30% probability level ellipsoids: (a) oblique view; (b) top view. Solvent molecules are omitted for clarity. Because of the small difference of electron density between nitrogen and carbon atoms and/or disorder of the *confused* pyrrole, the position of the peripheral nitrogen atom could not be determined. Here, one of the possible structures is shown.

Scheme 8. Preparation of **4**

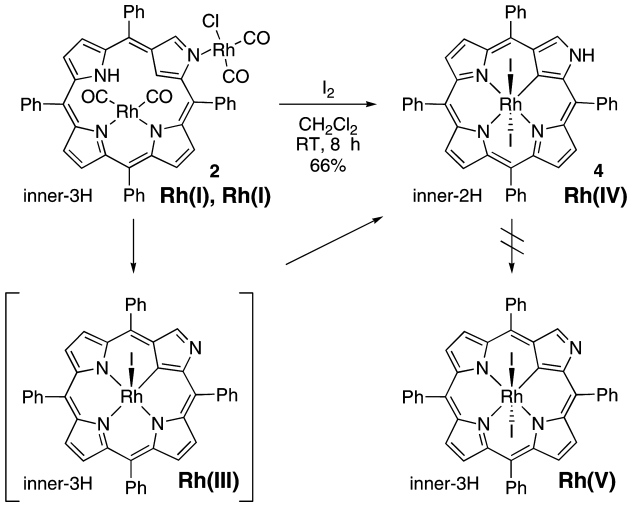

FAB mass analyses ($[M - I]^+ = 842$; $[M - 2I]^+ = 715$), structural assignment of **4** relies on the X-ray analysis and SQUID measurement.

The skeletal structure of **4** in a solid state was elucidated by the X-ray crystallographic analysis (Figure 5). The rhodium atom is placed in the center of the porphyrin core, and two iodine atoms are connected as axial ligands with an atomic distance of 2.6557(3) Å, which is slightly longer than that of the TPP Rh(III) complex **7** [2.6335(9) Å vide infra]. There is no counteranion in the crystal. In addition, the solvent EtOH molecule is located near the peripheral nitrogen atoms with an interatomic N−O distance of 2.703 Å, which suggests the presence of a NH hydrogen atom. While it was difficult to distinguish the rhodium oxidation states between rhodium(IV) (inner-2H, with the hydrogen atom attached to the peripheral

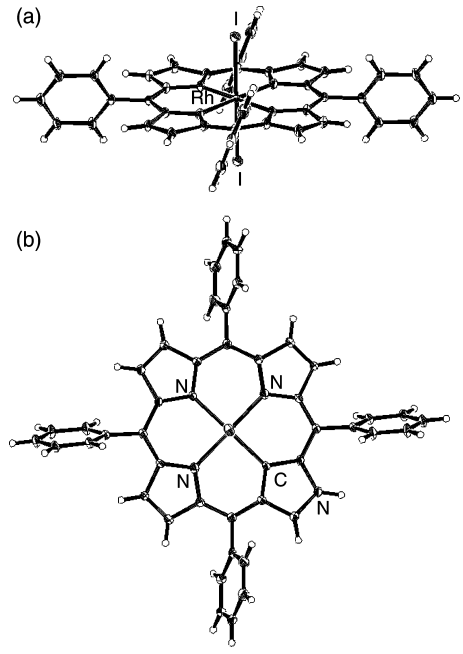

Figure 5. Molecular structures of **4**·EtOH with 30% probability level ellipsoids: (a) oblique view; (b) top view. Solvent molecules are omitted for clarity. Because of a small difference of electron density between nitrogen atoms and carbon atoms and/or disorder of the *confused* pyrrole, the position of the peripheral nitrogen atom could not be determined. Here, one of the possible structures is shown.

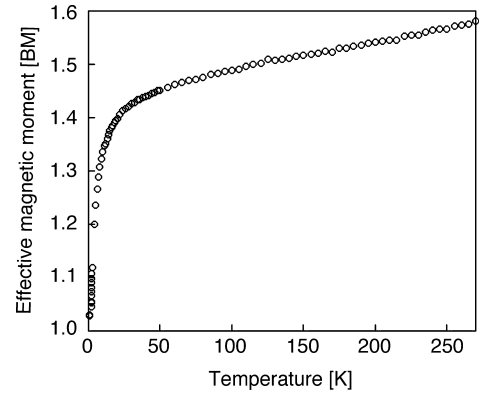

Figure 6. Temperature dependence on the effective magnetic moment of **4** in the solid state.

nitrogen atom) and rhodium(V) (inner-3H, with no hydrogen atom on the peripheral nitrogen atom) explicitly by the X-ray analysis, distinctive evidence was obtained by the SQUID measurement. Thus, when the NCP moiety has the inner-3H-type structure, the formal charge on the rhodium ion should be 5+ ($S = 0$). In contrast, the formal charge on the rhodium metal should be 4+ ($S = {}^1/_2$) in the case of the inner-2H structure. Because the SQUID measurement indicated that **4** had a paramagnetic character and the spin quantum number of **4** was estimated as $S = {}^1/_2$ (Figure 6), the inner-2H-type structure, that is, the formal oxidation state being 4+ for the rhodium metal, was inferred for **4** in the solid phase. Detection of an IR absorption signal assignable to the outer-NH moiety in the solid phase was so far unsuccessful possibly because of a weak intensity. Note that the corresponding outer-N-methylated derivative of **4**, which has an absorption spectrum similar to that of **4**, was obtained when the *N*-methyl-NCTPP was treated with $[RhCl(CO)_2]_2$ and then with I_2, although no reliable X-ray structure had been obtained yet (see the Supporting Information).

To obtain further information on the electronic state of the rhodium complex **4**, NMR and electron spin resonance (ESR) measurements were achieved in solution. Unexpectedly, no ^{1}H NMR signals have so far been detected between δ −310 and +310 ppm under the measuring conditions where the ^{1}H NMR signals for the paramagnetic nickel(II) complex of NCTPP were clearly observed.[31] While the reason for the absence of NMR signals is still unclear, one possibility might be the presence of an equilibrium among some electronic states like NCTPP Rh(IV) and NCTPP$^{\bullet+}$ Rh(III) in solution. The unique ESR spectrum of **4** also implied the existence of some electronic states (Figure 7). Although a complete understanding was difficult because of the complicated hyperfine and superhyperfine splittings due to multiple nuclei such as ^{103}Rh, ^{127}I, ^{14}N, and ^{1}H, the g values (1.968, 2.025, and 2.10) and the highly broadened signals suggested the predominant existence of a metal-centered spin state. Because reports on the paramagnetic rhodium(IV) complexes are extremely limited, a further discussion on the details of the rhodium oxidation state of **4** should be deferred at present.[32]

(31) Chmielewski, P. J.; Latos-Grażyński, L.; Głowiak, T. *J. Am. Chem. Soc.* **1996**, *118*, 5690.
(32) Feldman, I.; Nyholm, R. S.; Watton, E. *J. Chem Soc.* **1965**, 4724.

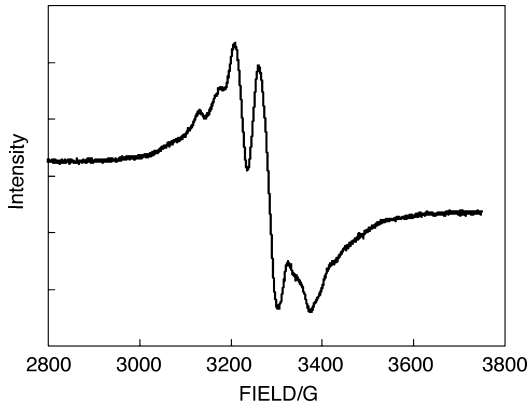

Figure 7. ESR spectrum of **4** in toluene at 77 K: concentration, 5.0×10^{-4} M; microwave power, 1 mW; modulation amplitude, 1.0 mT.

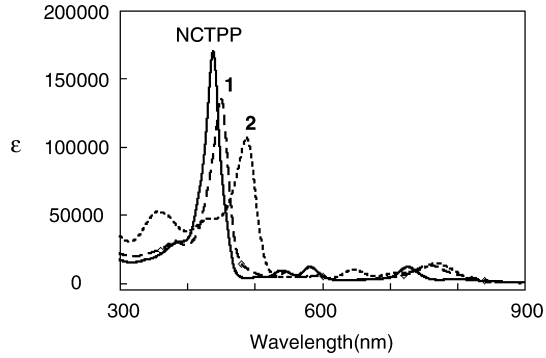

Figure 8. Absorption spectra of NCTPP mono-Rh(I) complex **1** and bis-Rh(I) complex **2** in CH_2Cl_2.

Absorption Spectrum. Peripheral coordination of a rhodium atom to NCTPP causes small red shifts in the UV/vis spectrum (Figure 8). The Soret-like band for the rhodium(I) complex **1** is observed at 450 nm, which is 12 nm red-shifted from the parent NCTPP (438 nm). The Q-type bands appear at 549, 593, and 758 nm and are red-shifted by 10−33 nm. This means that peripheral coordination does not disrupt facile π conjugation of the porphyrin ring. Similarly, in the case of meso-metalated porphyrins, ca. 10−20 nm red shifts were observed as compared to the parent porphyrins.[2b]

Unlike peripheral coordination, chelation of a rhodium metal to the inner nitrogen atoms causes a significant red-shift in the UV/vis spectrum, which is commonly observed in porphyrin metal complexes. The Soret-like band of the bisrhodium(I) complex **2** in CH_2Cl_2 is observed at 488 nm and, compared to the monorhodium(I) complex **1**, shows a 38 nm red shift. The Q-type bands appear in the region of 548−780 nm, which is further red-shifted from **1** in ca. 10 nm.

Absorption spectra of the rhodium(III) complex **3** and the rhodium(IV) complex **4** show rather different profiles, as shown in Figure 9. The rhodium(III) complex **3** keeps typical features of the porphyrin metal complex; the Soret-like band of **3** appears at 451 nm, and the Q-type bands appear at 538, 579, 668, 718, and 798 nm. In contrast, the absorption spectrum of **4** is rather deformed and resembles that of TPP bis-Rh(I) complex **6** (Figure 10). The Soret-like band is split into two peaks (351 and 478 nm), and no distinct Q-type bands are observed. Such a deformation of the UV/vis spectrum might be due to the

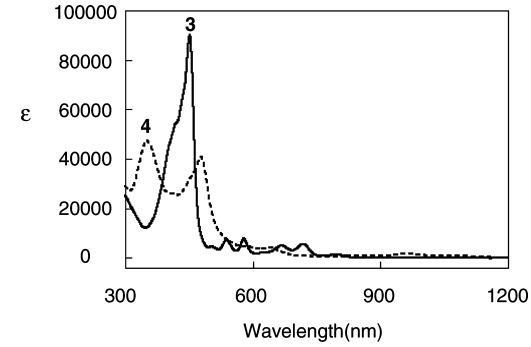

Figure 9. Absorption spectra of the rhodium(III) and -(IV) complexes (**3** and **4**) in CH_2Cl_2.

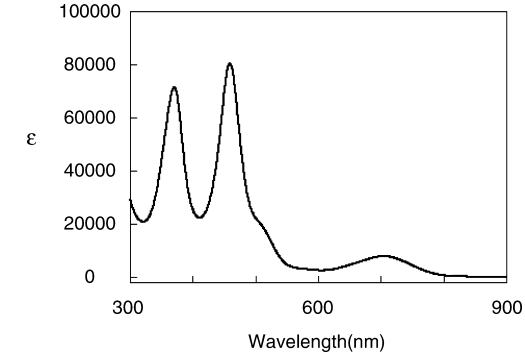

Figure 10. Absorption spectrum of TPP bis-Rh(I) complex **6** in CH_2Cl_2.

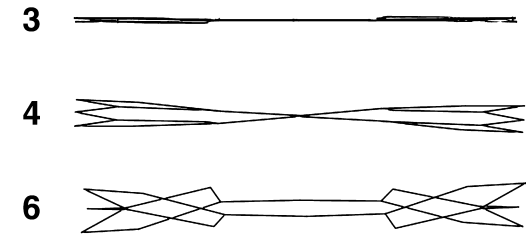

Figure 11. Side views of the solid-state structures for **3**, **4**, and **6**. Only 24 heavy atoms composing porphyrin rings are shown for clarity.

Scheme 9. Rhodium Chemistry of NCTPP and TPP

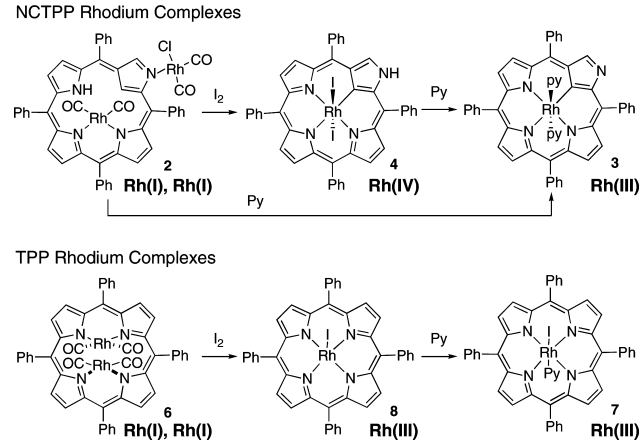

ruffled structures of the porphyrin planes (Figure 11). Note that $TPPRh^{III}$ complex **7** also shows the ruffled structure.[30]

The reactions of NCTPP afforded rhodium complexes that were comparable but different from those of TPP because of the flexible coordination of the NCTPP ligand (Scheme 9). As shown above, oxidation of the NCTPP bis-Rh(I) complex **2** with I_2 gave the NCTPP Rh(IV) complex **4**. In contrast,

oxidation of the TPP bis-Rh(I) complex **6** with I_2 gave not a rhodium(IV) complex but a TPP Rh(III) complex **8**, which had only one axial I_2 ligand.[33] These results suggested that NCTPP has a better ability to stabilize metal centers of higher oxidation state, which was possibly because of the large electronic donation from the confused pyrrole moiety to the metal center. Next, when the NCTPP Rh(IV) complex **4** was treated with pyridine, reduction of the metal center occurred to give the NCTPP Rh(III) complex **3**, which was also obtained by the reaction of **2** with pyridine. In the case of the TPP Rh(III) complex **8**, the reaction with pyridine caused only axial coordination to afford the TPP Rh(III) complex **7**.[30] While the mechanism of reduction was unclear, the reaction demonstrated that the NCTPP ligand could change its valence through protonation/deprotonation at the peripheral nitrogen moiety in harmony with the environment.[34]

Conclusion

In conclusion, a variety of NCTPP rhodium complexes were prepared, and their structures as well as fundamental properties were investigated. The NCTPP ligand shows a versatile coordination mode in rhodium chemistry and can form the rhodium(I), rhodium(III), and even rhodium(IV) complexes through NH tautomerism as well as distortion of the porphyrin plane. Such flexible coordination was never observed in the normal porphyrin case. Application of NCP rhodium complexes to catalyst[35,36] and investigation of their electronic states, especially for the rhodium(IV) complex, are now underway.

Experimental Section

General Procedures. All reactions were carried out under N_2 or Ar. All commercially available reagents were used as received. All ^{1}H NMR spectra were taken at 300 MHz and ^{13}C NMR spectra at 75 MHz (JEOL JNM-AL300). Spectra are reported in part per million from internal tetramethylsilane or the residual protons of the deuterated solvent for the ^{1}H NMR spectra and from the carbon signal of the deuterated solvent for the ^{13}C NMR spectra. IR spectra were recorded on a Jasco FT/IR-620 instrument; absorptions are reported in cm^{-1}. Mass spectra were measured with a JEOL JMS-T100CS (ESI mode) or JEOL-HX110 (FAB mode). UV/vis absorption spectra were recorded on a Shimadzu UV-3150PC spectrometer. Frozen-solution ESR spectra were taken at 77 K in quartz tubes with 4 mm inner diameter on a JEOL JES-RE1X X-band spectrometer equipped with a standard low-temperature apparatus. The *g* values were calibrated with a manganese(II) marker used as a reference.

Preparation of (NCTPP)RhCl(CO)$_2$ (1). A mixture of NCTPP (19.7 mg, 32.0 μmol) and [RhCl(CO)$_2$]$_2$ (6.4 mg, 16.5 μmol) in CH_2Cl_2 (20 mL) was stirred at 26 °C for 10 min. The resulting solution was concentrated to dryness under reduced pressure, and the residue was recrystallized from CH_2Cl_2/hexane to afford the rhodium(I) complex **1** as a greenish-brown powder (24 mg, 30 μmol, 93% yield): IR (KBr, CO) 2071, 1995 cm^{-1}; ^{1}H NMR ($CDCl_3$, 300 MHz) δ −4.64 (s, 1H, inner-CH), −1.81 (br s, 2H, inner-NH), 7.72−7.78 (m, 6H, Ph), 7.82−7.94 (m, 4H, Ph), 8.02 (t, J = 7.6 Hz, 2H, Ph), 8.10−8.18 (m, 4H, Ph), 8.30−8.34 (m, 2H, Ph), 8.43−8.48 (m, 2H + 2H, Ph + β-CH), 8.50 (d, J = 4.9 Hz, 1H, β-CH), 8.56 (d, J = 4.9 Hz, 1H, β-CH), 8.64 (s, 1H, α-CH), 8.87 (d, J = 4.9 Hz, 1H, β-CH), 8.97 (d, J = 4.9 Hz, 1H, β-CH); ^{13}C NMR ($CDCl_3$, 75 MHz) δ 93.74, 118.33, 118.98, 126.59, 126.76, 126.87, 127.17, 127.45, 128.01, 128.05, 128.52, 128.58, 128.68, 129.15, 129.24, 129.72, 129.94, 131.46, 134.54, 134.82, 135.35, 135.60, 136.81, 137.19, 137.63, 138.21, 138.82, 140.98, 141.07, 142.13, 142.38, 144.23, 154.54, 158.31, 158.60, 180.52 (d, $^1J_{Rh-C}$ = 72.2 Hz), 183.83 (d, $^1J_{Rh-C}$ = 66.6 Hz); UV/vis (CH_2Cl_2, λ_{max}/nm (ϵ)) 758 (13 000), 593 (5400), 549 (8100), 450 (140 000). HRMS (ESI$^+$). Found: *m*/*z* 809.12272. Calcd for $C_{46}H_{31}Cl_1N_4O_2Rh$ ([MH]$^+$): *m*/*z* 809.11906.

Preparation of (NCTPP)Rh(CO)$_2$Rh(CO)$_2$Cl (2). NCTPP (50 mg, 81 μmol) was dissolved in CH_2Cl_2 (50 mL). Anhydrous sodium acetate (67 mg, 810 μmol, 10 equiv) and [Rh(CO)$_2$Cl]$_2$ (32 mg, 81 μmol, 1.0 equiv) were added to the solution, and the mixture was stirred under reflux for 2 h. The solvent was evaporated, and the residue was separated by chromatography on a silica gel column with CH_2Cl_2/CH_3OH (99:1). Removal of the solvent gave the NCTPP bis-Rh(I) complex **2** as a blue-green solid, which was recrystallized from CH_2Cl_2/hexane (42 mg, 43 μmol, 53% yield). Because **2** was slowly decomposed at ambient temperature in solution, it was so far difficult to obtain reliable ^{13}C NMR data: IR (KBr, CO) 2075, 2010, 1993 cm^{-1}; ^{1}H NMR ($CDCl_3$, 300 MHz): δ −3.83 (s, 1H, inner-CH), 0.11 (br s, 1H, inner-NH), 7.72−7.75 (m, 6H), 7.89−7.91 (m, 4H), 7.95−8.08 (m, 4H), 8.10−8.20 (m, 4H), 8.27 (d, J = 5.0 Hz, 1H), 8.33 (d, J = 4.0 Hz, 2H), 8.48 (d, J = 5.0 Hz, 1H), 8.53 (d, J = 3.0 Hz, 1H), 8.59 (d, J = 2.0 Hz, 1H), 8.78 (d, J = 7.0 Hz, 1H), 8.90 (s, 1H, outer-CH), 8.97 (dd, J = 2.0 and 7.0 Hz, 1H); MS (FAB$^+$) *m*/*z* 967 ([MH]$^+$); UV/vis (CH_2Cl_2, λ_{max}/nm (ϵ)) 770 (14 300), 646 (9700), 589 (5300), 548 (4500), 488 (110 000), 433 (47 000), 358 (53 000). Anal. Calcd for **2**·0.5CH_2Cl_2·0.5H_2O: C, 57.19; H, 3.07; N, 5.50. Found: C, 57.65; H, 3.44; N, 5.47.

Preparation of Rh(NCTPP)(py)$_2$ (3). The bisrhodium(I) complex **2** (61.0 mg, 62.9 μmol) was dissolved in 30 mL of pyridine and stirred at 19 °C for 10 min. The resulting solution was concentrated to dryness under reduced pressure, and the residue was subjected to silica gel column separation (eluent: CH_2Cl_2/MeOH = 99/1 and then THF). The THF fraction was evaporated, and the solid thus obtained was recrystallized from CH_2Cl_2/hexane to give the NCTPP Rh(III) complex **3** as a brown solid (28.7 mg, 32.9 μmol, 52% yield): ^{1}H NMR ($CDCl_3$, 300 MHz) δ 2.36 (br d, J = 5.2 Hz, 4H, *o*-py), 5.35 (distorted t, J ∼ 7.0 Hz, 4H, *m*-py), 6.23 (distorted t, J ∼ 7.5 Hz, 2H, *p*-py), 7.59−7.66 (m, 12H, Ph), 7.96−8.09 (m, 8H, Ph), 8.23 (d, J = 4.6 Hz, 1H, β-CH), 8.25 (d, J = 4.9 Hz, 1H, β-CH), 8.28 (d, J = 4.6 Hz, 1H, β-CH), 8.29 (d, J = 4.9 Hz, 1H, β-CH), 8.42 (d, J = 4.9 Hz, 1H, β-CH), 8.54 (d, J = 4.9 Hz, 1H, β-CH), 9.16 (s, 1H, α-CH); ^{13}C NMR ($CDCl_3$, 75 MHz) δ 115.67, 118.07, 121.86, 126.41, 126.48, 126.57, 126.62, 126.84, 126.91, 126.98, 128.21, 129.07, 129.46, 130.16, 130.23, 130.62, 131.52, 133.79, 133.87, 134.01, 134.20, 134.32, 139.20, 141.08, 141.31, 141.62, 141.70, 141.80, 143.06, 143.15, 143.77, 143.81, 148.22, 149.00 (d, $^1J_{Rh-C}$ = 26.8 Hz), 166.14; UV/vis (CH_2Cl_2, λ_{max}/nm (ϵ)) 798 (1500), 718 (5700), 668 (5000), 579 (7800), 538 (7200), 451 (90 000). HRMS (ESI$^+$). Found: *m*/*z* 873.22295. Calcd for $C_{54}H_{38}N_6Rh$ ([MH]$^+$): *m*/*z* 873.22130.

Preparation of Rh(NCTPP)I$_2$ (4). To a solution of NCTPP (50 mg, 81 μmol, 1.0 equiv) in 40 mL of CH_2Cl_2 was added I_2 (20 mg, 79 μmol, 0.98 equiv), and the mixture was stirred at ambient temperature for 8 h. The resulting slurry was washed with an aqueous KI solution and brine. After removal of the solvent, the residue was chromatographed on silica gel with CH_2Cl_2/hexane to give the NCTPP Rh(IV) complex **4** (52 mg, 54 μmol, 66% yield): UV/vis (CH_2Cl_2,

(33) Callot, H. J.; Schaeffer, E. *Nouv. J. Chim.* **1980**, *4*, 311.
(34) Maeda, H.; Ishikawa, Y.; Matsuda, T.; Osuka, A.; Furuta, H. *J. Am. Chem. Soc.* **2003**, *125*, 11822.
(35) (a) Callot, H. J.; Piechocki, C. *Tetrahedron Lett.* **1980**, *21*, 3489. (b) Huang, L.; Chen, Y.; Gao, G.-Y.; Zhang, X. P. *J. Org. Chem.* **2003**, *68*, 8179.
(36) Niino, T.; Toganoh, M.; Andrioletti, B.; Furuta, H. *Chem. Commun.* **2006**, 4335.

Table 3. Crystal Data and Structure Analysis Results for Rhodium Complexes **2**−**4** and **6**

	2·0.5CH_2Cl_2·0.5H_2O	**3**·2CH_3CN	**4**·EtOH	**6**·CH_2Cl_2
formula	$C_{48.50}H_{31}Cl_2N_4O_{4.5}Rh_2$	$C_{58}H_{44}N_8Rh$	$C_{46}H_{34}I_2N_4ORh$	$C_{49}H_{30}Cl_2N_4O_4Rh_2$
cryst syst	monoclinic	triclinic	triclinic	monoclinic
space group	*C*2/*c* (No. 15)	$P\bar{1}$ (No. 2)	$P\bar{1}$ (No. 2)	*C*2/*c* (No. 15)
R, R_w [$I > 2\sigma(I)$]	0.0357, 0.0454	0.0468, 0.0563	0.0375, 0.0409	0.0355, 0.0642
R1, wR2 (all data)	0.1192, 0.1146	0.1031, 0.1072	0.0947, 0.0974	0.0761, 0.0812
GOF	1.054	1.071	1.073	0.967
a, Å	18.0381(3)	9.1793(8)	9.1089(7)	21.695(2)
b, Å	31.4290(5)	10.489(1)	11.315(1)	11.1778(7)
c, Å	17.1686(3)	11.868(2)	11.717(1)	21.600(1)
α, deg	90	80.28(1)	64.512(2)	90
β, deg	111.3050(6)	79.748(7)	86.478(5)	120.957(3)
γ, deg	90	84.367(8)	66.596(4)	90
V, Å^3	9068.0(3)	1105.6(2)	991.6(2)	4492.0(5)
Z	8	1	1	4
μ, cm^{-1}	8.93	4.37	20.28	9.00
T, K	296(2)	123(2)	123(2)	296(2)
cryst size, mm	0.90 × 0.20 × 0.15	0.30 × 0.10 × 0.08	0.25 × 0.15 × 0.08	0.10 × 0.10 × 0.10
D_{calcd}, g cm^{-3}	1.492	1.436	1.700	1.501
$2\theta_{min}$, $2\theta_{max}$, deg	3.6, 50.0	4.8, 50.0	4.2, 52.0	4.3, 51.0
no. of rflns measd (unique)	8010	3706	3788	4186
no. of rflns measd [$I > 2\sigma(I)$]	6493	3340	3523	3036
no. of param	537	305	260	281
transmn factors T_{min}, T_{max}	0.600, 0.878	0.880, 0.966	0.631, 0.855	
Δ, e Å^{-3}	1.08, −0.49	0.60, −0.48	1.54, −0.70	0.78, −0.61

λ_{max}/nm (ϵ)) 957 (1700), 854 (980), 478 (41 000), 351 (47 000); MS (ESI$^+$) *m*/*z* 842 ([M − I]$^+$). Anal. Calcd for **4**·EtOH: C, 54.41; H, 3.37; N, 5.52. Found: C, 54.65; H, 3.41; N, 5.26.

Preparation of Rh(NCTPP)(py)$_2$Rh(CO)$_2$Cl (5). A mixture of **3** (15.2 mg, 17.4 μmol) and $[RhCl(CO)_2]_2$ (3.7 mg, 9.5 μmol) in CH_2Cl_2 (15 mL) was stirred at 23 °C for 3 h. The resulting solution was concentrated to dryness under reduced pressure, and the residue was recrystallized from CH_2Cl_2/MeOH to afford **5** as a brown powder (18.0 mg, 16.9 μmol, 97% yield): IR (KBr, CO) 2068, 1992 cm^{-1}; ^{1}H NMR ($CDCl_3$, 300 MHz) δ 2.60 (t, J = 5.5 Hz, 4H, py), 5.46 (t, J = 6.9 Hz, 4H, py), 6.25−6.36 (m, 2H, py), 7.61−7.75 (m, 11H, Ph), 7.75−8.04 (m, 8H, Ph), 8.13 (d, J = 4.9 Hz, 1H, β-CH), 8.21−8.24 (s overlapped with d, 1H + 2H, β-CH), 8.34 (d, J = 7.6 Hz, 1H, Ph), 8.38 (d, J = 4.9 Hz, 1H, β-CH), 8.43 (d, J = 4.9 Hz, 1H, β-CH), 9.09 (s, 1H, α-CH); ^{13}C NMR ($CDCl_3$, 75 MHz) δ 116.23, 118.59, 122.21, 122.38, 126.43, 126.57, 126.70, 126.76, 126.86, 126.90, 126.99, 127.23, 127.26, 127.33, 127.62, 127.67, 128.26, 129.11, 129.41, 130.22, 131.07, 131.16, 131.43, 131.58, 132.47, 133.78, 133.87, 133.93, 134.14, 134.58, 134.88, 136.71, 139.68, 139.92, 140.41, 141.23, 142.37, 142.47, 143.22, 143.40, 143.81, 144.93, 145.67, 147.83 (d, $^1J_{Rh-C}$ = 27.4 Hz), 148.22, 148.42, 166.46, 181.43 (d, $^1J_{Rh-C}$ = 76.6 Hz), 184.79 (d, $^1J_{Rh-C}$ = 66.0 Hz).

Preparation of (TPP)[Rh(CO)$_2$]$_2$ (6). TPP (50 mg, 81 μmol, 1.0 equiv) was dissolved in 50 mL of CH_2Cl_2. Anhydrous sodium acetate (67 mg, 810 μmol, 10 equiv) and $[Rh(CO)_2Cl]_2$ (32 mg, 81 μmol, 1.0 equiv) were added to the solution, and the mixture was stirred at reflux for 2 h. The solvent was evaporated under reduced pressure, and the residue was separated by chromatography on a silica gel column with hexane/CH_2Cl_2 (30:70, v/v). Removal of the solvent gave the TPP bis-Rh(I) complex **6** as a purple solid, which was recrystallized from CH_2Cl_2/hexane (27 mg, 29 μmol, 36% yield): ^{1}H NMR ($CDCl_3$, 300 MHz) δ 7.79−7.82 (m, 12H), 8.28−8.34 (m, 8H), 8.57 (d, J = 4.5 Hz, 4H), 8.73 (d, J = 4.5 Hz, 4H); MS (FAB$^+$) *m*/*z* 931 ([MH]$^+$); UV/vis (CH_2Cl_2, λ_{max}/nm (ϵ)) 704 (7900), 460 (80 000), 371 (71 000). Anal. Calcd for **6**: C, 61.95; H, 3.03; N, 6.02. Found: C, 61.69; H, 3.07; N, 6.05.

X-ray Crystallography. Crystals of **2**−**4** and **6** suitable for a X-ray diffraction study were mounted on a Rigaku RAXIS RAPID imaging-plate area detector with graphite-monochromated Mo Kα radiation. Crystal data and data statistics are summarized in Table 3. The structures were solved by the direct methods of *SHELXS-97* and refined using the *SHELXL-97* program.[37] The non-hydrogen atoms except for some solvent molecules were refined anisotropically by the full-matrix least-squares method. Hydrogen atoms were refined using the riding model. The CCDC reference numbers are 164092 (**2**), 610986 (**3**), 610987 (**4**), and 164093 (**6**).

Magnetic Susceptibility Measurement. Static magnetic susceptibility data were obtained from 270 to 1.9 K on a Quantum Design MPMS5S magnetometer and corrected for magnetization of the sample holder and capsule and for diamagnetic contributions (−400−10^{-6} emu mol^{-1}) to the samples, which were estimated from Pascal's constants.[38] Data were recorded at 50 kG on a sample of 46.53 mg.

Acknowledgment. This research was supported by a Grant-in-Aid for Scientific Research (Grant 16350024) from Monbukagaku-sho, Japan, and PRESTO from JST, Japan. We thank Dr. Yuichi Shimazaki and Dr. Satoru Karasawa for their help in the ESR and SQUID measurements of **4**, respectively.

Supporting Information Available: Crystal data for **2**−**4** and **6** in CIF format, preparation of Rh(N-Me-NCTPP)I_2, and UV/vis spectra of Rh(NCTPP)I_2 and Rh(N-Me-NCTPP)I_2. The material is available free of charge via the Internet at http://pubs.acs.org.

IC061093+

(37) Sheldrick, G. M. *Program for the Solution of Crystal Structures*; University of Göttingen: Göttingen, Germany, 1997.
(38) Kahn, O. *Molecular Magnetism*; Wiley-VCH Publishers: Weinheim, Germany, 1993.